Study of Multibody Aerodynamic Interference at Transonic Mach Numbers

Charles J. Cottrell* and Agusto Martinez†
U. S. Air Force Armament Laboratory, Eglin Air Force Base, Florida
and
Gary T. Chapman‡
NASA Ames Research Center, Moffett Field, California

A wind-tunnel experiment involving single, double, and triple combinations of mutually interfering generic, unfinned aircraft stores has been conducted. Each combination of stores was tested at Mach numbers from 0.60 to 1.20, and at angles of attack from 0 to 25 deg for the single store and from 0 to 6 deg for the double- and triple-store configurations. Extensive axial and circumferential pressure and flow visualization data at each store location were obtained. Euler solutions for each configuration at 0 deg incidence have been generated and compared with experimental data. This comparison indicates that an Euler flow solver can yield accurate predictions of the location and magnitude of multibody interference provided an appropriate grid is used and the viscous effects associated with these configurations remain small. The data indicate that multibody interference in the transonic region increases as the freestream Mach number approaches 1 from either direction, and subsides as the Mach number moves away from sonic conditions. This interference is characterized by a large, localized reduction in pressure on the inboard surfaces of the bodies, which results in forces that draw the configuration closer together.

Nomenclature

C_p = pressure coefficient, $(P-P_\infty)/(\frac{1}{2}\rho_\infty V_\infty^2)$
C_p^* = pressure coefficient for $M=1$
D = model diameter, 2.54 cm (1 in.)
L = model length, 15.09 cm (5.94 in.)
M_∞ = freestream Mach number
P = static pressure
P_∞ = freestream static pressure
V_∞ = freestream velocity
X = axial location measured from nose tip
α = angle of attack
β = angle of yaw
ρ_∞ = freestream density
ϕ = circumferential angle

Introduction

THE mutual aerodynamic interference of aircraft stores in external carriage has long been of interest to the aerodynamicist. It is widely recognized that both aircraft survivability and mission effectiveness are dependent on aerodynamic forces generated by stores in carriage. This is particularly true in the transonic Mach range, conditions where stores are often carried and where the resulting flowfields are complex and difficult to resolve. The potential of computational fluid dynamics (CFD) to predict accurately forces and moments acting on mutually interfering bodies is progressing at a fast pace.[1-4] The advent of high-speed supercomputers with large memory gives the aerodynamicist the means to employ Euler and Navier-Stokes flow solvers to investigate the complex fluid interactions that occur around multibody configurations.

It is recognized that a comprehensive experimental data base is required to guide and verify these CFD efforts. Unfortunately, existing data are not of a generic nature and often involve geometric complexities, which may render them inappropriate for influencing the step-by-step evolution of these CFD codes and algorithms. Results from a recently completed set of wind tunnel experiments provide pressure and flow visualization data around mutually interfering generic-shaped stores in multiple component configurations at transonic Mach numbers for CFD code validation.

The purpose of this paper is to use a portion of these experimental results along with Euler flow solver predictions to study mutual aerodynamic interference involving two- and three-store configurations at transonic conditions

Model and Test Conditions

The experiment was conducted in the Arnold Engineering Development Center PWT-4T wind tunnel. The model consisted of one-, two-, and three-store combinations of a generic store consisting of a 3.333 diam cylindrical centerbody and a 1.667 diam tangent ogive forebody and afterbody, with the afterbody truncated to mount to a sting (Fig. 1a). The distance between the stores was 0.8 diam for the two- and three-body configurations (Fig. 1b). This spacing was chosen arbitrarily and was not intended to simulate a specific aircraft store loading. Only one store was instrumented. It had a total of 87 pressure taps consisting of three longitudinal rows of 29 orifices located by 120 deg increments around its circumference. The instrumented store was rotated to measure pressure at 10 deg intervals around its circumference, as shown in Fig. 1b. The instrumented model was moved to similarly record pressure data at each store position for the two- and three-body configurations. Details of the three-body configuration mounted in the wind tunnel test section are shown in Fig. 2.

Each configuration was tested at $M_\infty = 0.60$, 0.85, 0.95, 1.05, and 1.20 with a freestream unit Reynolds number main-

Presented as Paper 87-0519 at the AIAA 25th Aerospace Sciences Meeting, Reno, NV, Jan. 12–15, 1987; received Jan. 20, 1987; revision received Nov. 9, 1987.

*Chief, Plans and Programs Office, Aeromechanics Division. Senior Member AIAA.
†Captain, U. S. Air Force, Aeromechanics Division. Member AIAA.
‡Senior Staff Scientist, Thermosciences Division. Associate Fellow AIAA.

tained at approximately 2.4×10^6/ft for all cases. The maximum test section blockage was less than 1%, well within recommended tunnel tolerance. Every configuration was tested at angles of attack α equal to 0, 2, 4, and 6 deg at 0 deg yaw β. In addition, the single store was tested at $\alpha = 10$, 15, 20, and 25 deg at $\beta = 0$ deg, and the two-store configuration was tested at $\alpha = 0$ deg with $\beta = 10$ deg. Oil flow visualization photographs were obtained following acquisition of the pressure data.

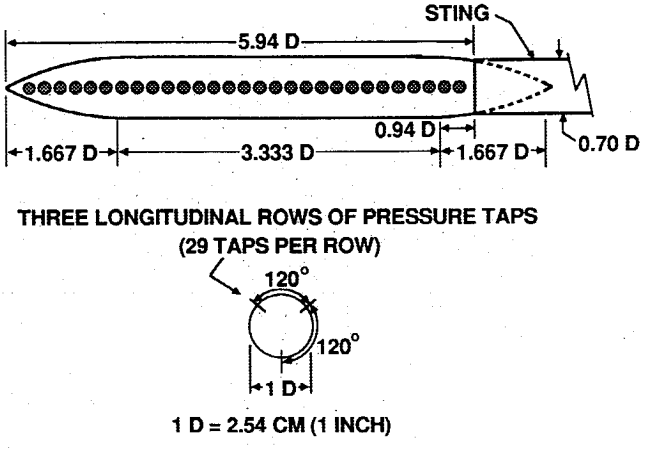

Fig. 1a Wind-tunnel model geometry.

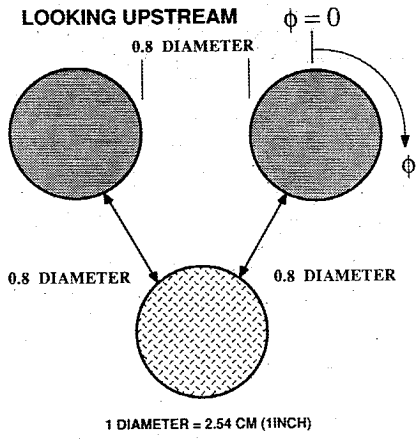

Fig. 1b Two- and three-store configuration alignment.

Euler Flow Solvers

Two Euler flow solvers were used to predict the pressure distributions on the three different configurations at 0 deg angle of attack. The first solver[2] was used for the single- and double-store configurations. A more robust solver[5] was required for the triple-store configurations. Both solvers use an explicit, upwind finite-volume scheme and are second order in both time and space. Both solve the flux-vector-split form of the Euler equations with local time-stepping and a Courant number less than 2 for steady-state computations.

The difference between the two Euler solvers is in the mechanism for computing the eigenvalues on the grid cell faces. The first code computes the eigenvalues by extrapolating the dependent variable,[2] whereas the second solver computes them by averaging the dependent variables.[5] These eigenvalues are used to determine the upwind direction. Reference 6 provides a direct comparison of both techniques. Characteristc variable boundary conditions[6] were used by both solvers on far-field boundaries and at the body surfaces. Reflection planes were used to simulate the two- and three-store configurations. Because of the use of these symmetry planes, pressure predictions were made from $\phi = 280$ deg clockwise to $\phi = 80$ deg for the two-store case, and from $\phi = 250$ deg clockwise to $\phi = 50$ deg (right-shoulder store) for the three-store configuration. Both solvers used an H-type algebraic grid generator that produced a $100 \times 10 \times 10$ grid around each of the configurations. A side view and a frontal view of the grid used for the triple-store configuration are presented in Figs. 3a and 3b, respectively.

Results and Discussion

The quality of the experimental pressure data, as represented by the pressure coefficient C_p, is addressed in Figs. 4a and 4b. Figure 4a shows surface pressure distributions along the body taken at three circumferential positions, 120 deg apart, for the single body at $\alpha = \beta = 0$ deg. The data from each circumferential location overlays that from the other two, thereby demonstrating both model and flow symmetry. Figure 4b serves to verify the model alignment for the three-body combination. Data taken on the right-shoulder store of the triple-store configuration at the circumferential angles $\phi = 210$ and 270 deg show excellent agreement. Since the double configuration would be indentical to this triple configuration with the bottom store removed, this alignment verification is assumed to hold for the two-body configuration as well.

The effect of Mach number on the mutual aerodynamic interference occurring around the bodies is presented in Figs. 5a–5c for $\alpha = 90$ deg and an outboard circumferential location of $\phi = 90$ deg. As demonstrated by the close agreement with the single-store data in Fig. 5a, there is little mutual interference for the two- and three-body combinations at

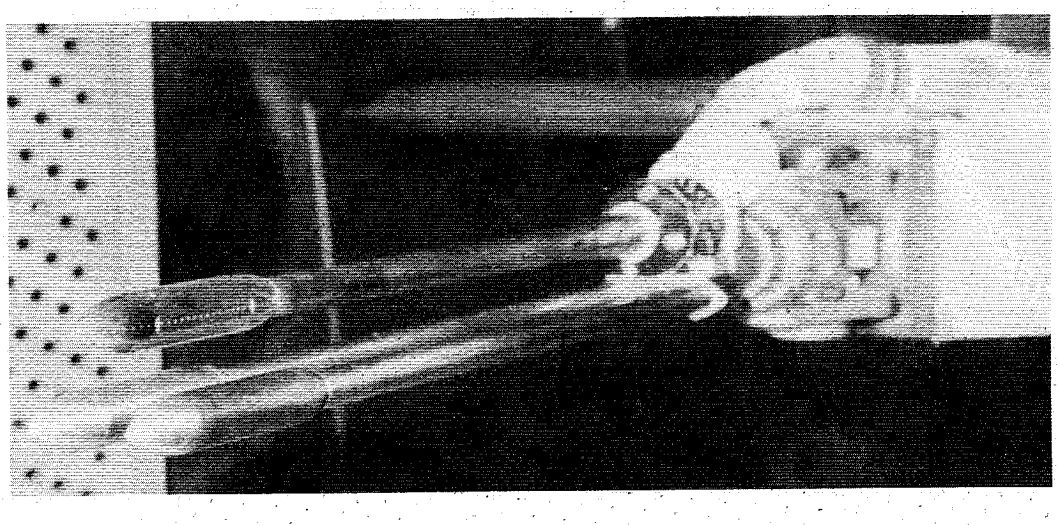

Fig. 2 Three-store model installation.

$M_\infty = 0.60$. However, the corresponding pressure data at $M_\infty = 0.95$ (Fig. 5b) indicate the presence of significant multibody interference. The interference commences at the forward shoulder and extends for approximately two-thirds the length of the cylinder. The existence of this mutual interference corresponds primarily to an increase in the length of the supersonic region for the multiple-store cases. The presence of a second store pushes the shock further back on the body, and the addition of a third store pushes it back further. Figure 5c shows that there is little mutual interference at $M_\infty = 1.20$ along the $\phi = 90$ deg circumferential angle. What interference exists commences near the middle of the cylinder and terminates near the aft ogive juncture where the flow undergoes an expansion. No imbedded shocks are present for any of the three configurations.

The effect of Mach number $\alpha = \beta = 0$ deg for an inboard circumferential location denoted at $\phi = 270$ deg is shown in Figs. 6a–6c. The amount of interference present at $M_\infty = 0.060$ and $\phi = 270$ deg (Fig. 6a), though small, is somewhat greater than that experienced at the $\phi = 90$ deg position. This is not surprising since the region between the stores would be expected to be most influenced by the proximity of the other store(s). However, the multibody interference demonstrated for $M_\infty = 0.95$ at this inboard location (Fig. 6b) is substantially more than the corresponding interference at the outboard position (Fig. 5b). Here, the shocks have strengthened considerably, but occur slightly forward of those for the outboard location. This has the effect of concentrating a stronger interference in a more narrow region of the cylinder than for the outboard position. Figure 6c demonstrates the extent of mutual interference at $M_\infty = 1.20$ along the $\phi = 270$ deg meridian. Here, the interference begins at the nose tip and is much larger than at the outboard position. This interference in the nose region may be due to the bow shock being pushed further upstream due to an increase in blockage as additional stores are added to the configuration. This has the effect of broadening the subsonic region near the nose. The addition of stores also causes the recompression along the aft portion of the cylinder to become stronger.

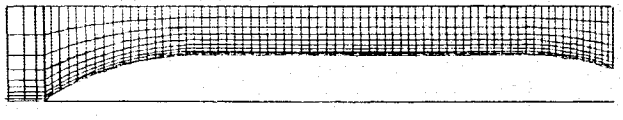

Fig. 3a Side view of three-store grid.

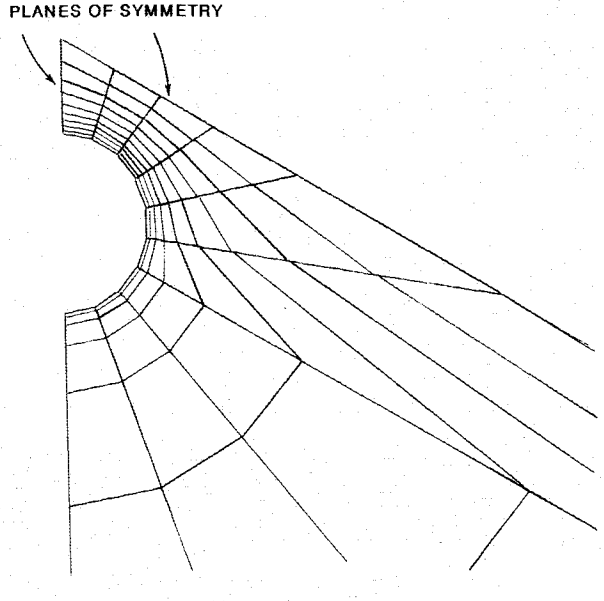

Fig. 3b Front view of three-store grid.

Figure 7 shows the circumferential pressure distribution at $M_\infty = 0.95$ ($\alpha = \beta = 0$ deg) on each of the three configurations at 42% of the axial length, as measured from the nose ($X/L = 0.420$). This axial location was chosen because it corresponds to a region of large interference. As expected, the circumferential pressure distribution is constant around the single store. The double configuration experiences maximum interference in the vicinity of $\phi = 270$ deg, the closest location to the second store. The right-shoulder store of the triple configuration undergoes maximum interference in the vicinity of $\phi = 240$ deg, which corresponds to the symmetry plane between the other two bodies. Minimum interference for the double and triple configurations occurs at $\phi = 90$ deg and $\phi = 60$ deg, respectively. Both locations are diametrically opposite to the maximum interference meridians discussed above.

Figure 7 also indicates that the flow is subsonic at $XL = 0.420$ for the single store. However, the presence of additional bodies causes the flow to become supersonic at this axial plane. It is important to note that this increase in Mach number corresponds to a lowering of pressure between/among the stores. This low pressure is most pronounced in the mid-cylinder region of the double- and triple-store combinations (Fig. 6b) and will exert a strong force pulling the bodies toward each other and possibly a moment. These forces and moments could cause problems if a store were to be released from these multibody configurations. This low-pressure region also has a strong effect on the axial boundary-layer flow, as will be discussed below.

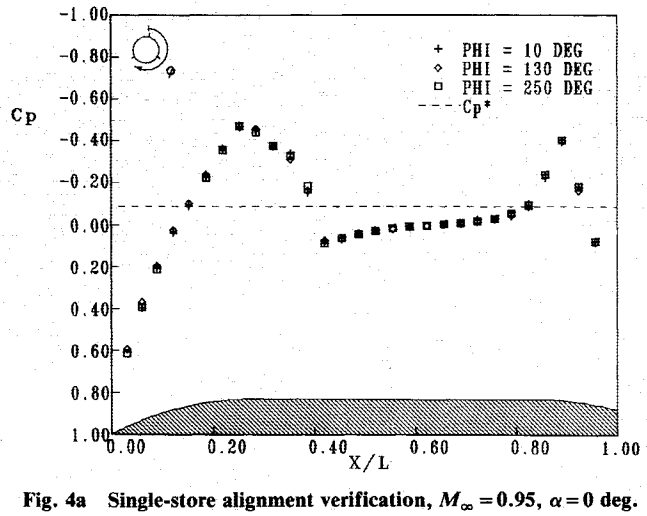

Fig. 4a Single-store alignment verification, $M_\infty = 0.95$, $\alpha = 0$ deg.

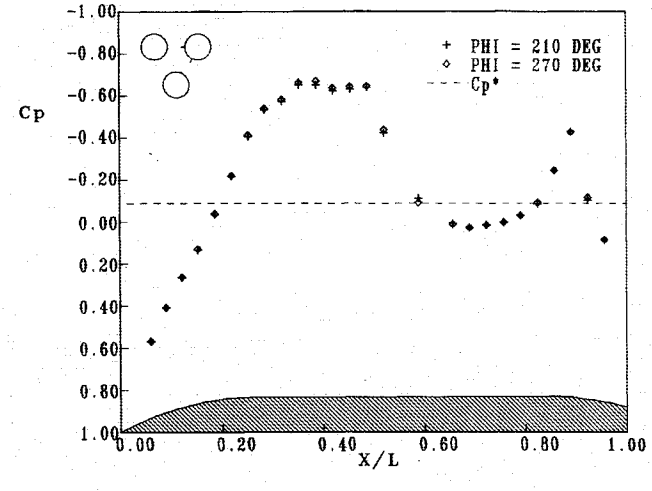

Fig. 4b Multistore alignment verification, $M_\infty = 0.95$, $\alpha = 0$ deg.

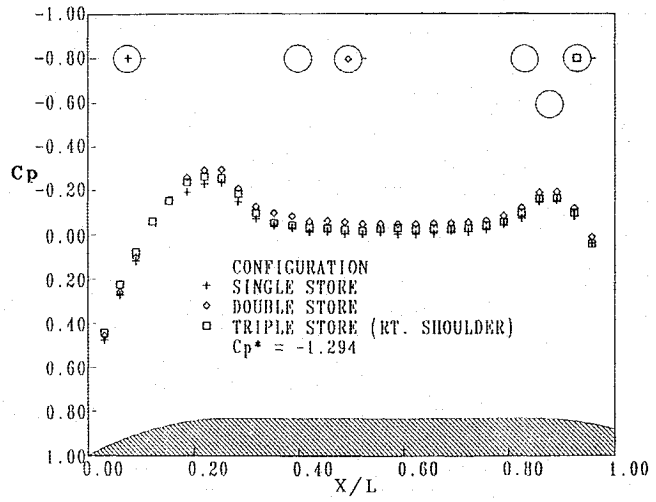

Fig. 5a Mutual interference comparison, $M_\infty = 0.60$, $\alpha = 0$ deg, $\phi = 90$ deg.

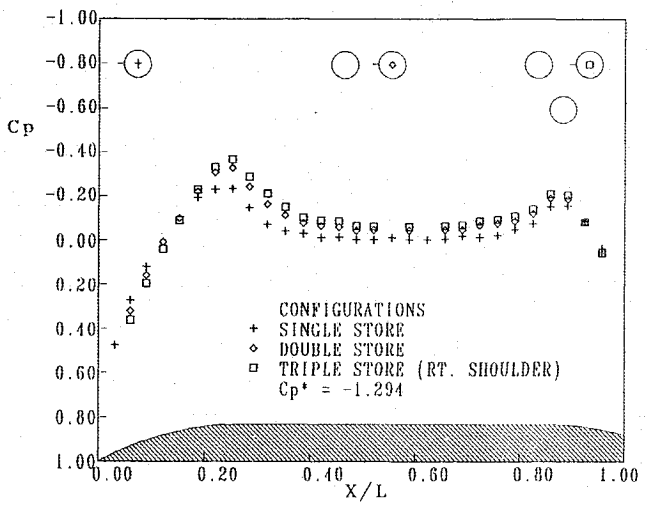

Fig. 6a Mutual interference comparison, $M_\infty = 0.60$, $\alpha = 0$ deg, $\phi = 270$ deg.

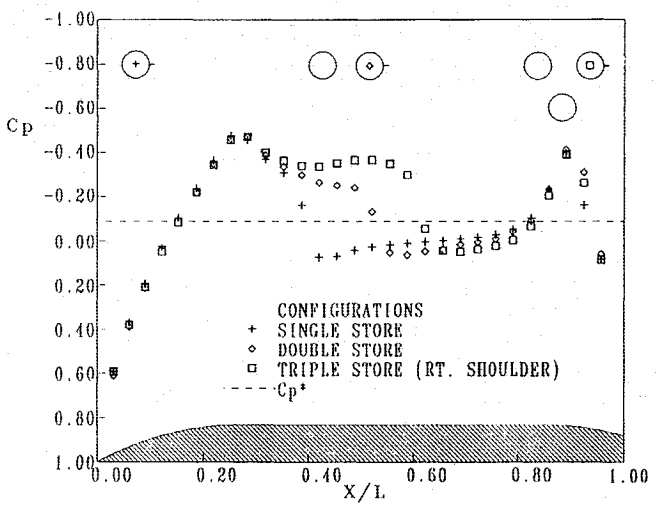

Fig. 5b Mutual interference comparison, $M_\infty = 0.95$, $\alpha = 0$ deg, $\phi = 90$ deg.

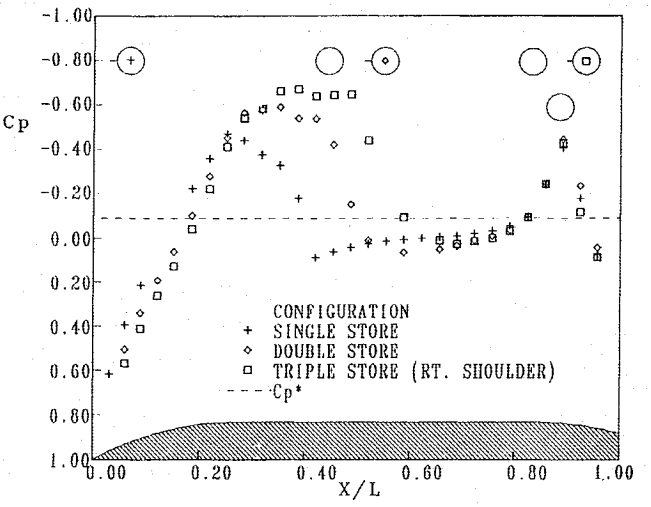

Fig. 6b Mutual interference comparison, $M_\infty = 0.95$, $\alpha = 0$ deg, $\phi = 270$ deg.

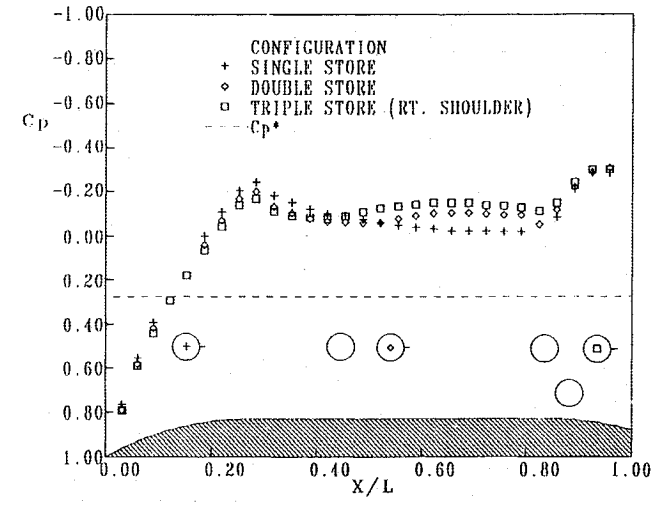

Fig. 5c Mutual interference comparison, $M_\infty = 1.20$, $\alpha = 0$ deg, $\phi = 90$ deg.

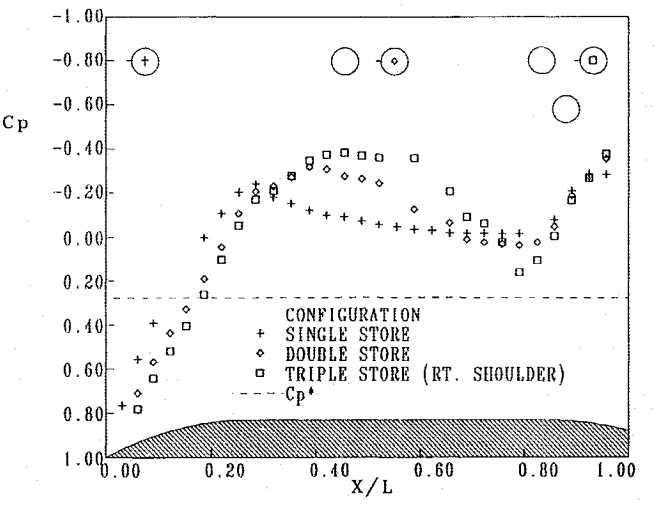

Fig. 6c Mutual interference comparsion, $M_\infty = 1.20$, $\alpha = 0$ deg, $\phi = 270$ deg.

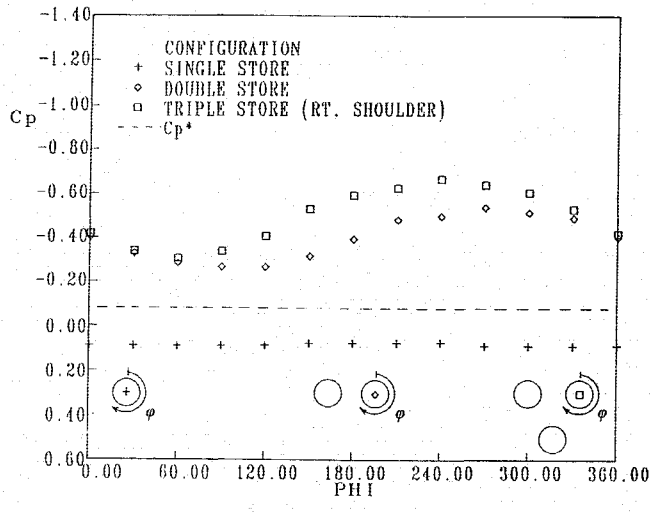

Fig. 7 Circumferential comparison, $M_\infty = 0.95$, $\alpha = 0$ deg, $X/L = 0.420$.

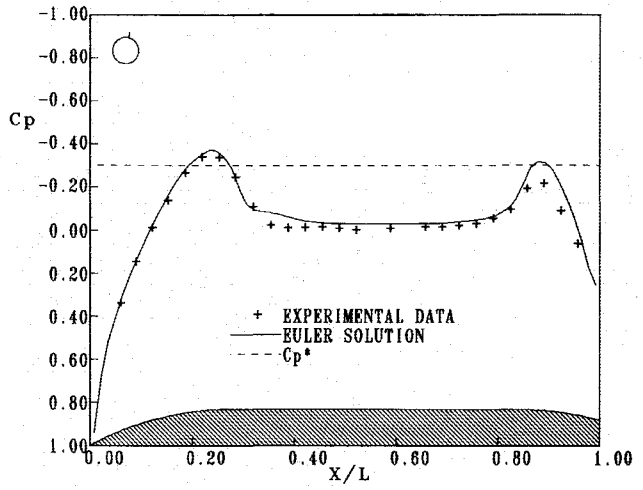

Fig. 8a Single-store experimental and numerical comparison, $M_\infty = 0.85$, $\alpha = 0$ deg, $\phi = 10$ deg.

Figures 8a–8c demonstrate the comparison between experimental data and Euler predictions for the single-, double-, and triple-store combinations, respectively, at $M_\infty = 0.85$, $\alpha = 0$ deg. The agreement for the single store is very good, as shown in Fig. 8a. Slight over-prediction of the flow expansion by the flow solver in the boat-tail region may be due to a combination of the inviscid nature of the code, coupled with the possibility of flow separation in this region. The comparison remains good for the double-store configuration (Fig. 8b) at the $\phi = 280$ deg position, near the position of maximum interference. Though mutual interference is high along this ray, the code provides a reasonable prediction of the pressure distribution. The solution has some difficulty in defining the exact location of the forward shoulder shock. However, it accurately resolves the magnitude of the minimum pressure occurring at the shoulder. The solution overpredicts the boat-tail expansion, as noted earlier. Figure 8c provides a comparison of experimental and Euler results for the triple configuration at $\phi = 270$ deg on the right-shoulder store, again near the position of maximum interference. The generally good comparison follows the trends discussed for the double-store configuration. However, the triple-store Euler prediction shows some "ringing" aft of the shock. The predicted shock is also slightly forward of the experimental data. The reason for this is not clearly understood but may be due to the coarseness of the grid.

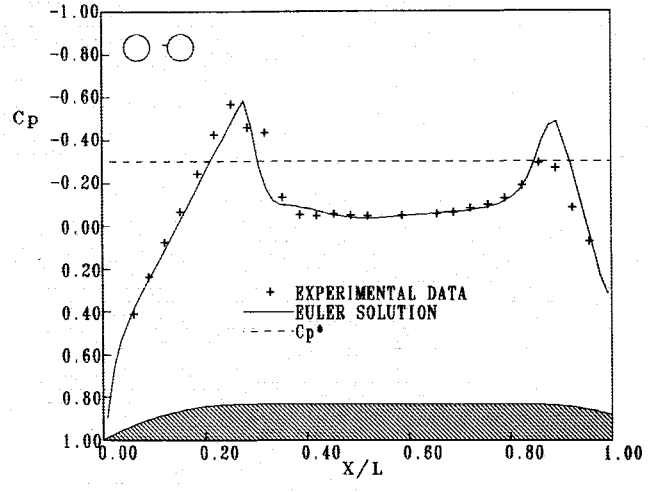

Fig. 8b Double-store experimental and numerical comparison, $M_\infty = 0.85$, $\alpha = 0$ deg, $\phi = 280$ deg.

Figures 9a–9e show the comparison between experimental data and Euler predictions for the three configurations at $M_\infty = 0.95$, $\alpha = \beta = 0$ deg. As was the case at $M_\infty = 0.85$, the flow solver provides very good agreement with the single store (Fig. 9a). However, the overprediction of the expansion in the boat tail region has become more pronounced. This is due to the higher Mach number and to the inviscid nature of the flow solver. The presence of strong viscous regions at the boat tail and at the shoulder are graphically demonstrated by the oil flow photograph (Fig. 10a). Figure 9b shows the comparison for the double configuration at $\phi = 80$ deg near the position of minimum interference. The agreement, though excellent at the nose, begins to break down at the forward shoulder. Figure 9c demonstrates the comparison for the same configuration at $\phi = 280$ deg near the maximum interference position. For this inboard location, agreement begins to break down slightly forward of the nose juncture. The double-store oil flow photograph presented in Fig. 10b shows a possible reason for this departure. The low-pressure region between the stores causes extensive boundary-layer flow into this region. This will lead to a thicker than normal boundary layer at this inboard location, and possibly to a small area of separation between $X/L = 0.35$ and 0.43. This thicker boundary layer and small

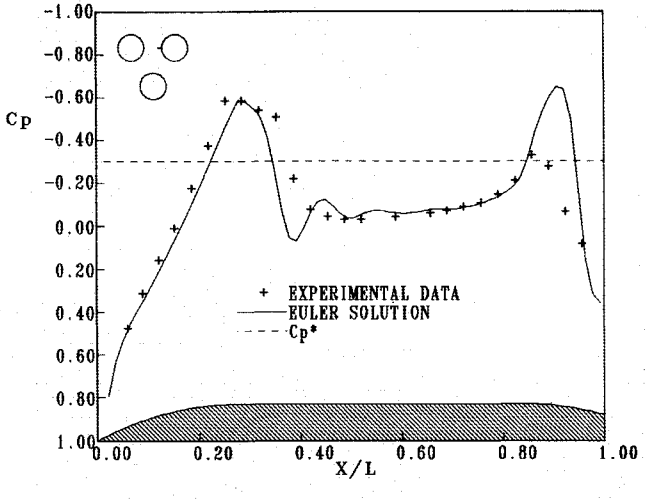

Fig. 8c Triple-store experimental and numerical comparison, $M_\infty = 0.85$, $\alpha = 0$ deg, $\phi = 270$ deg.

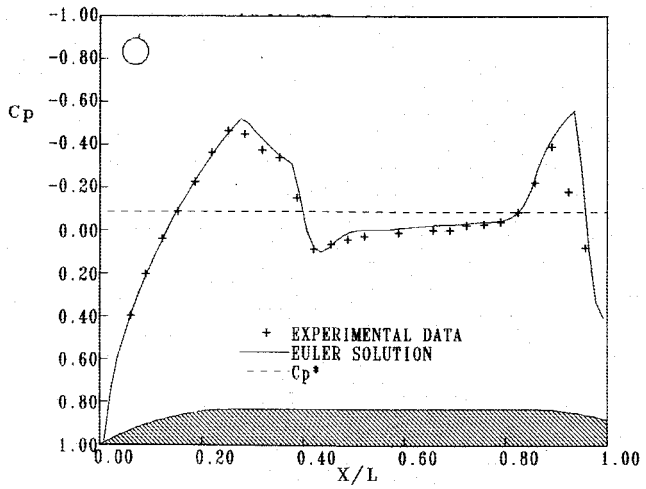

Fig. 9a Single-store experimental and numerical comparison, $M_\infty = 0.95$, $\alpha = 0$ deg, $\phi = 10$ deg.

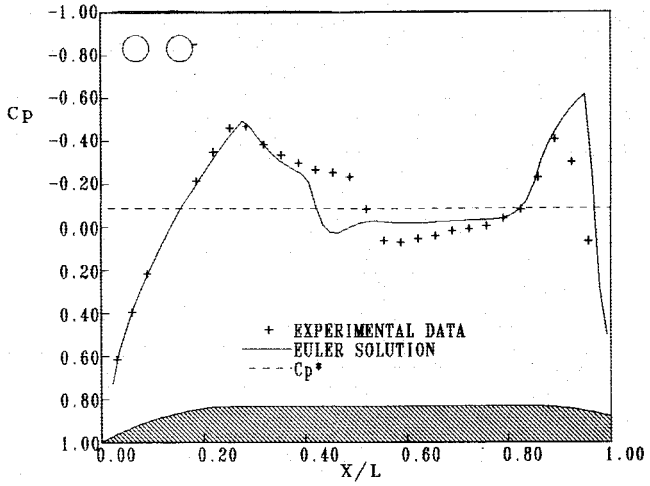

Fig. 9b Double-store experimental and numerical comparison, $M_\infty = 0.95$, $\alpha = 0$ deg, $\phi = 80$ deg.

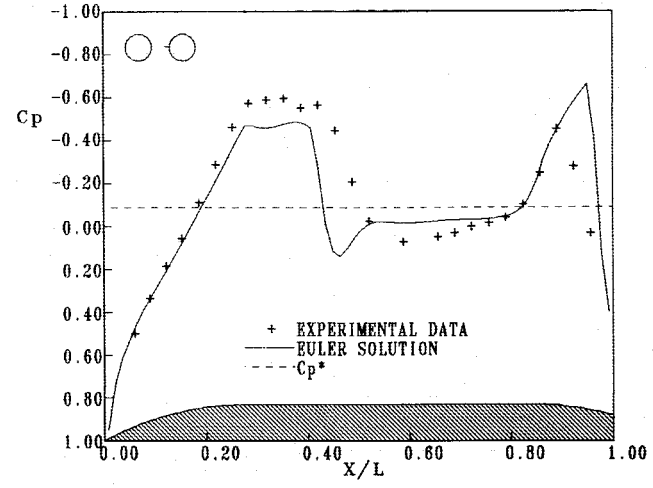

Fig. 9c Double-store experimental and numerical comparison, $M_\infty = 0.95$, $\alpha = 0$ deg, $\phi = 280$ deg.

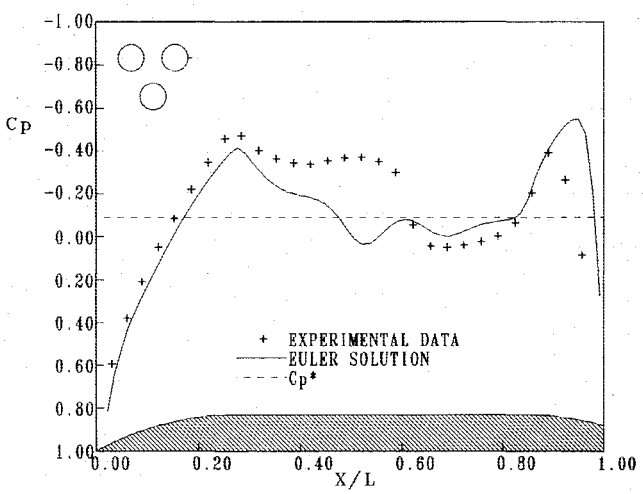

Fig. 9d Triple-store experimental and numerical comparison, $M_\infty = 0.95$, $\alpha = 0$ deg, $\phi = 90$ deg.

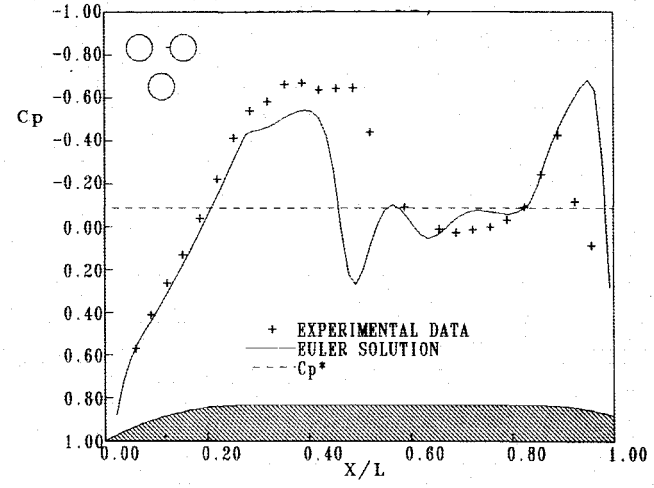

Fig. 9e Triple-store experimental and numerical comparison, $M_\infty = 0.95$, $\alpha = 0$ deg, $\phi = 270$ deg.

separation results in additional constriction of the flow and, hence, the lower pressure than predicted by the Euler code.

Figure 9d presents the comparison for the triple configuration at $\phi = 90$ deg on the right-shoulder store. Agreement is poor along most of this circumferential location. For this case, the predicted pressures begin diverging from the experimental results near the nose tip. Comparison is also poor for the right-shoulder store along the inboard location $\phi = 270$ deg (Fig. 9e). The predicted location of the shock is too far forward. Figures 10c and 10d show the oil flow results for the triple configuration as viewed from below and above, respectively. Here, again, one sees the rapid movement of the boundary-layer flow toward the inboard location, and the oil flow patterns also show some evidence of separation on both inboard and outboard surfaces. These thicker boundary layers and the small separation at the inboard location constrict the flow and result in a lower pressure and a longer supersonic zone than predicted by the Euler code.

In summary, the Euler predictions compare favorably with the experimental data for those conditions where viscous effects are small. The strong viscous effects produced by the mutual interference at $M_\infty = 0.95$ are clearly evident in the oil flow photographs in Figs. 10b–10d.

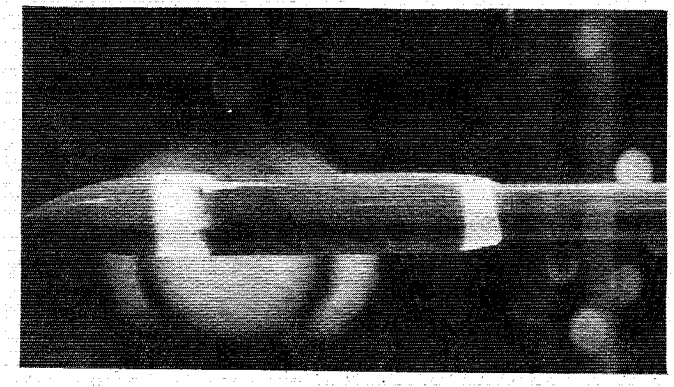

Fig. 10a Single-store oil flow, $M_\infty = 0.95$, $\alpha = 0$ deg.

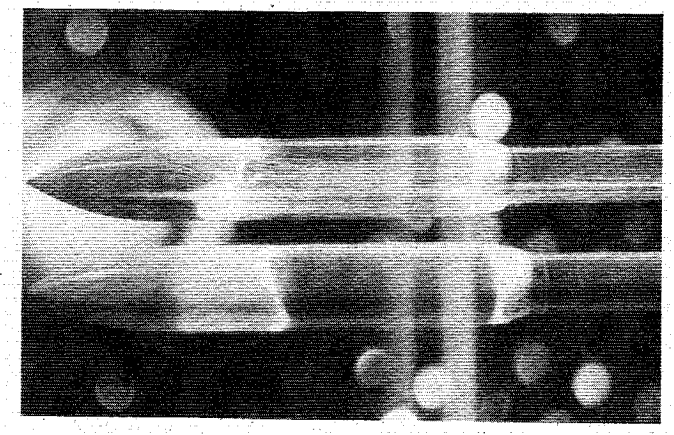

Fig. 10b Double-store oil flow, $M_\infty = 0.95$, $\alpha = 0$ deg.

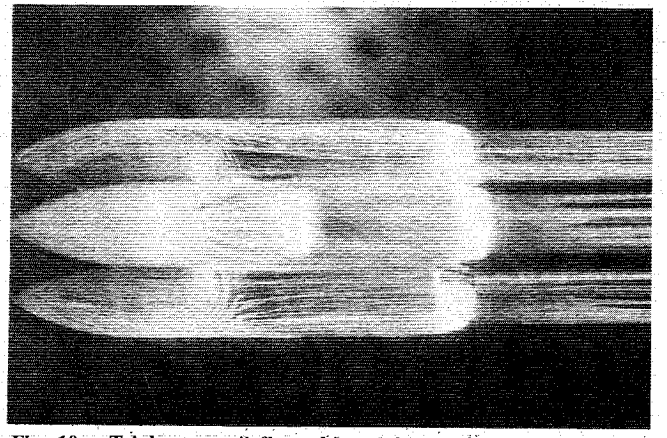

Fig. 10c Triple-store oil flow, $M_\infty = 0.95$, $\alpha = 0$ deg (viewed from "below").

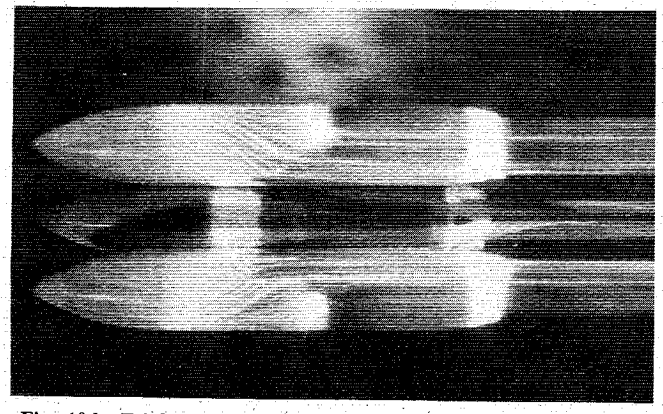

Fig. 10d Triple-store oil flow, $M_\infty = 0.95$, $\alpha = 0$ deg (viewed from "above").

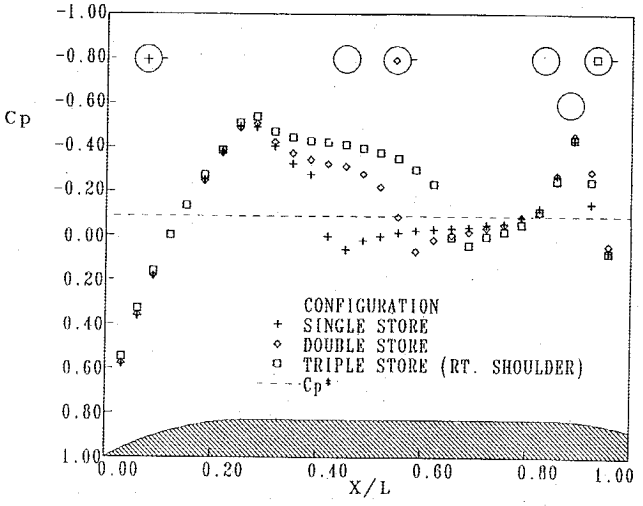

Fig. 11a Mutual interference comparison, $M_\infty = 0.95$, $\alpha = 6$ deg, $\phi = 90$ deg.

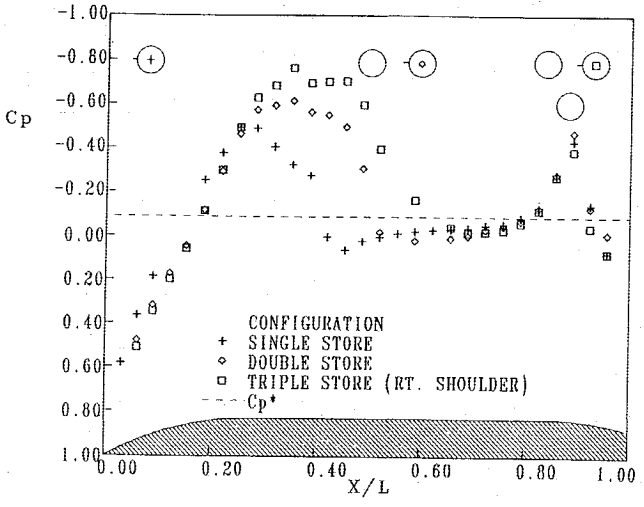

Fig. 11b Mutual interference comparison, $M_\infty = 0.95$, $\alpha = 6$ deg, $\phi = 270$ deg.

So far, the discussion has focused on the interference generated in the flow by the proximity of multiple bodies at zero incidence. Figures 11a and 11b show the effect of mutual interference at $\alpha = 6$ deg for three configurations at $M_\infty = 0.95$, $\beta = 0$ deg. Figure 11a shows the interference at $\phi = 90$ deg. The magnitude of the interference at this outboard location is almost identical to that of the zero incidence case (see Fig. 5b). Similar results for the inboard position, $\phi = 270$ deg, are presented in Fig. 11b. Here, too, there is only a small change in the magnitude of interference as compared to the $\alpha = 0$ deg case (Fig. 6b).

The oil flow photographs shown as Figs. 12a–12d confirm that the interference occurring on the multistore configurations seems to be more dependent on the proximity of the bodies than on the incidence of the configuration. Figures 12a and 12b show the double-store oil flow photographs for the windward and leeward surfaces, respectively. There are no significant differences in the flow patterns between either the windward or leeward surfaces and the pattern presented in Fig. 10b for $\alpha = 0$ deg. Similarly, Figs. 12c and 12d, respectively, show the oil flow results for the windward and leeward surfaces of the triple-store configuration. Here, too, there are no significant differences in the flow patterns compared to those at zero incidence (Figs. 10c and 10d, respectively). A small change is the occurrence of two spots of accumulated oil

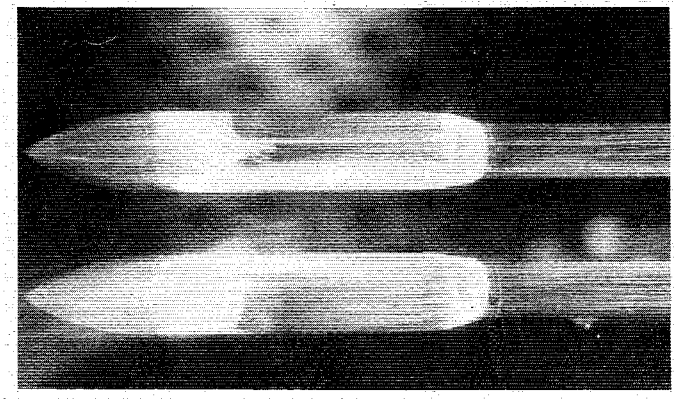

Fig. 12a Double-store oil flow, $M_\infty = 0.95$, $\alpha = 6$ deg (windward surface).

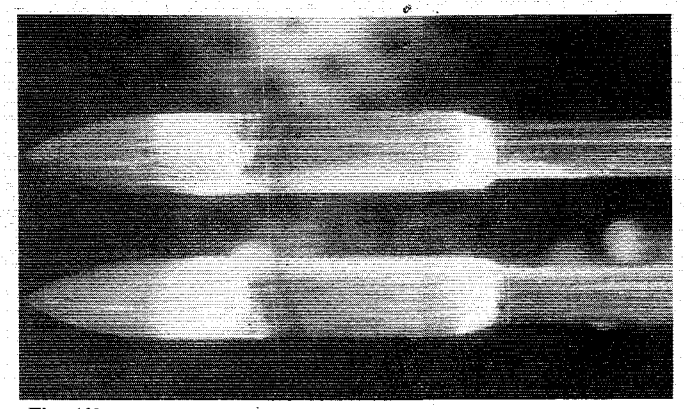

Fig. 12b Double-store oil flow, $M_\infty = 0.95$, $\alpha = 6$ deg (leeward surface).

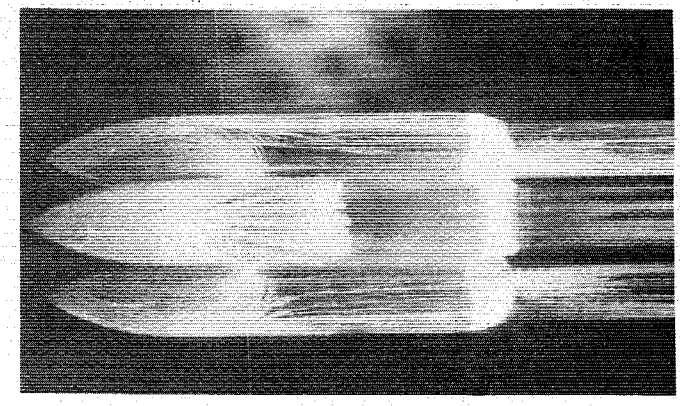

Fig. 12c Triple-store oil flow, $M_\infty = 0.95$, $\alpha = 6$ deg (windward surface).

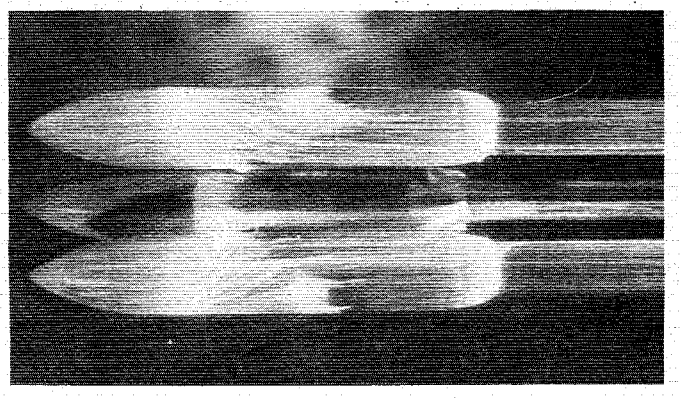

Fig. 12d Triple-store oil flow, $M_\infty = 0.95$, $\alpha = 6$ deg (leeward surface).

on the leeward surfaces ($X/L \simeq 0.5$). These appear to indicate the origin of vortices that are present for this lifting condition.

Concluding Remarks

A study of multibody aerodynamic interference based on recently obtained experimental data and CFD prediction has been performed. The following conclusions can be drawn.

1) Multibody interference in the transonic region is greatest at freestream Mach numbers near 1. This interference subsides as the freestream Mach number increases or decreases away from sonic conditions.

2) This interference is characterized by a large, localized reduction in pressure on the inboard surfaces of the bodies. This low pressure results in significant boundary-layer flow toward these surfaces. The low pressure also results in forces that act to draw the configuration closer together. It could impart a moment to an individual body being separated from a multibody configuration and, thereby, adversely affect the separation of a store from a parent aircraft.

3) The change of the multibody interference due to a configuration incidence of 6 deg or less is negligible when compared to that generated by the proximity of the bodies.

Finally, it is recognized that viscous effects would increase if the stores were placed closer together, the angle of attack were increased, or a pylon were added to a configuration. As a consequence, the Euler prediction might become less accurate. However, it was concluded that an Euler flow solver can provide accurate predictions of multibody interference as long as an appropriate grid is used and the viscous effects associated with these configurations remain small.

References

[1]Lijewski, L. E., Thompson, J. F., and Whitfield, D. L., "Computational Fluid Dynamics for Weapon Carriage and Separation," AGARD Symposium on Store Airframe Aerodynamics, AGARD Paper No. 3, Oct. 1985.

[2]Belk, D. M., Janus, M. J., and Whitfield, D. L., "Three-Dimensional Unsteady Euler Equations Solutions on Dynamic Grids," AIAA Paper 85-1704, July 1985.

[3]Doughtery, F. C., Benek, J. A., and Steger, J. L., "On Application of Chimera Grid Schemes to Store Separation," NASA TM-881193, Oct. 1985.

[4]Janus, J.M., "The Development of a Three-Dimensional Split Flux Vector Euler Solver with Dynamic Grid Applications," M. S. Thesis, Mississippi State Univ., Mississippi State, MS, 1984.

[5]Whitefield, D. L. and Janus, J. M., "Three-Dimensional Unsteady Euler Equations Solution Using Flux Vector Splitting," AIAA Paper 84-1552, June 1984.

[6]Mounts, J. S., Hughson, M. C., and Belk, D. M., "A Numerical Investigation of Finite Volume Techniques Using the Inviscid Burgers Equation," Air Force Armament Laboratory, Eglin AFB, FL, AFATL TR-86-66, Oct. 1986.